PHOTONICS Research

Build-up dynamics in bidirectional soliton fiber lasers

Igor Kudelin,[1] Srikanth Sugavanam,[1] and Maria Chernysheva[2,*]

[1]Aston Institute of Photonics Technologies, Aston University, Aston Triangle, Birmingham B4 7ET, UK
[2]Leibniz Institute of Photonics Technology, Albert-Einstein srt. 9, Jena 07745, Germany
*Corresponding author: maria.chernysheva@leibniz-ipht.de

Received 27 January 2020; revised 13 March 2020; accepted 14 March 2020; posted 16 March 2020 (Doc. ID 388988); published 6 May 2020

Bidirectional ultrafast fiber lasers present an attractive solution, enabling the generation of two mutually coherent ultrashort pulse trains in a simple and turnkey system. Still, the lack of a comprehensive numerical model describing steady-state bidirectional generation, and even less ultrafast soliton breakdowns and collisions, is obstructing the achievement of the performance compared with unidirectional lasers. In this paper, we have experimentally investigated real-time build-up dynamics of counter-propagating solitons in an ultrafast ring Er-doped fiber laser via the dispersive Fourier transform methodology. We parade that counter-propagating pulses experience independent build-up dynamics from modulation instability, undergoing breathing dynamics and diverging subordinate pulse structure formation and annihilation to a stable bidirectional pulse train. Yet, the interaction of pulses in the cavity presents the key underlying phenomenon driving formation evolution distinct from unidirectional pulse build-up. Our findings will provide physical foundations for bidirectional ultrafast fiber laser design to carry forward their application.

https://doi.org/10.1364/PRJ.388988

1. INTRODUCTION

The field of ultrafast photonics and technology over the past years has experienced a new rise of research interest in the fundamental studies of ultrafast pulse evolution dynamics. High-precision real-time measurements have been enabled by recent progress in modern electronics, unveiling and experimentally exploring the variety of ultrafast processes, including instabilities [1], rogue waves [2], soliton molecule evolution [3,4], breathing structures [5], and build-up dynamics of dissipative solitons and solitons-similaritons in fiber lasers [6–8]. Dispersive Fourier transform (DFT) [9] and time lens [2,10,11] techniques rely on the stretching of pulse temporal intensity waveforms in dispersive media. Provided that the dispersion is large enough to fulfill the far-field condition, the stretched waveform in the time domain will represent its spectral intensity. Therefore, these techniques allow recording the evolution of the single-shot optical spectra of pulses in the time domain over round trips. To look inside the fine temporal dynamics with a resolution of several hundreds of femtoseconds, one can perform the fast Fourier transformation of recorded spectra to convert them into field autocorrelation traces according to the Wiener–Khinchin theorem [7].

Nevertheless, all previously demonstrated works had a sharp focus on conventional mode-locked Ti:sapphire or unidirectional fiber lasers, and studied pulse interactions such as repulsion and attraction or phase change in co-propagating soliton complexes, e.g., soliton molecules [3,12]. Undoubtedly, robust unidirectional laser systems are capable of generation of high-power ultrashort pulses with unprecedented stability for industrial applications. Compared to them, the field of bidirectional lasers is not currently mature and cannot claim such performance. Bidirectional laser cavities have received the initial research interest with the demonstration of colliding mode-locking in dye lasers [13]. The scientific attention in bidirectional mode-locking has been reinforced [14,15] with the high demand for ultrafast laser ring gyroscopes in metrology [16,17] and coherent dual-comb generation for spectroscopy [18]. Still, the lack of study of underlying soliton dynamics presents a significant restriction toward the advancement of bidirectional ultrafast laser generation and its applications. However, the unique physics of bidirectional fiber lasers are rich with nonlinear phenomena over the collision of counter-propagating solitons and the interaction with counter-propagating dispersive waves. These optical effects were scantily studied experimentally [16,19], while considered theoretically only outside laser cavities [20,21].

In this work, we use the DFT technique to record the real-time spectral dynamics of counter-propagating solitons during their formation in an isolator-less mode-locked fiber laser. Both solitons undergo formation from modulation instabilities through spectral breathing and pulse splitting with segregation of a single peak, forming a stable generation pattern in each

direction. Such build-up dynamics, though at first glance resembles pulse formation in unidirectional lasers [6,7], is strongly affected by pulse collision in the cavity. More importantly, our findings expose the difference in spectral evolution dynamics for counter-propagating solitons, which has not been studied previously. These results shed light on the further understanding of nonlinear dynamics in bidirectional soliton systems and other complex systems with colliding and interacting pulses.

2. EXPERIMENTAL SETUP

The experimental setup for bidirectional soliton generation is a passively mode-locked erbium-doped fiber laser, sketched in Fig. 1, adopted from Ref. [15]. Mode-locking relies on the single-walled carbon nanotube saturable absorber (SWNT) and nonlinear polarization evolution technique, based on polarizing fiber. Nonlinear polarization evolution allows tuning the nonlinear transfer function by simple adjustment of polarization controllers, thus modifying the interactions of counter-propagating pulses and changing their optical paths. The laser operates in the anomalous dispersion regime, producing near-transform-limited pulses of 790 and 570 fs duration, respectively, for the clockwise and counter-clockwise channel, at 14.7 MHz repetition rate (round-trip time of 68 ns). Time-bandwidth products are 0.37 for clockwise and 0.335 for counter-clockwise pulses, correspondingly.

A 3 dB coupler combines counter-propagating pulses for consistent and synchronous analysis. The lengths of input ports of the coupler were adjusted by insertion of a ∼6 m long section of passive fiber (single-mode fiber), as shown in Fig. 1, to separate counter-propagating pulses by ∼30 ns and, therefore, avoid overlapping of spectral profiles during stretching in the DFT line. One output port of the coupler is used for measuring the evolution of instantaneous intensity $I(t)$ over N round trips. The signal from the other port is transmitted through

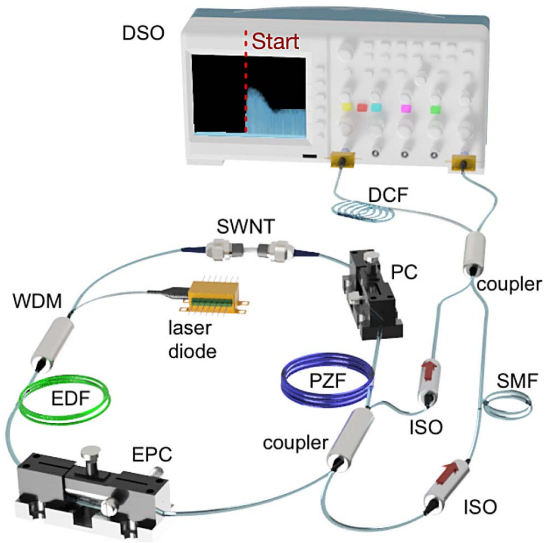

Fig. 1. Experimental setup. EDF, Er-doped fiber; WDM, wavelength-division multiplexer; SWNT, single-walled carbon nanotubes; PC, polarization controller; EPC, electronic polarization controller; PZF, polarizing fiber; ISO, isolator; SMF, single-mode fiber; DCF, dispersion compensating fiber; DSO, digital storage oscilloscope.

an ∼11 km long normal dispersion compensating fiber to stretch optical pulses and convert the temporal profile into spectral via DFT. Two 50 GHz photodetectors (Finisar XPDV2320R) were used to capture data and record it using a 33 GHz digital storage oscilloscope (Agilent). The temporal delay between spatiotemporal and single-shot spectral measurements is ∼53.6 μs. The temporal and spectral resolutions are 30 ps and 0.28 nm, correspondingly [7].

In our experiments, first, polarization controllers were adjusted to achieve stable mode-locked generation in two directions. By slight detuning of the electronically driven polarization controller, yet preserving the pump power at the same level, the laser switched to noise-like continuous-wave operation. The digital storage oscilloscope was triggered to make a single measurement when the bidirectional generation was achieved via tuning of the polarization controller to its initial position. We measured multiple oscilloscope data sequences demonstrating common stages of build-up dynamics of counter-propagating pulses from CW background to their stable state. The recorded oscilloscope data was processed into sequences of single-shot spectra using the information of round-trip time and counter-propagating pulses time separation. The single-shot spectra of counter-propagating pulses in the steady state of mode-locking are in a good agreement with average spectra measured by an optical spectrum analyzer (from Yokogawa) [15,17]. The relation between the spectral $\Delta\lambda$ and the temporal Δt domains has been mapped as $\Delta t = |D|L\Delta\lambda$, where $|D|$ and L are the dispersion and length of the DFT line.

3. RESULTS AND DISCUSSION

Figures 2(a) and 2(c) demonstrate the experimental results on typical formation dynamics of clockwise and counter-clockwise pulses recorded over the entire build-up process using the DFT technique. Since the time-bandwidth product of generated soliton pulses is close to the Fourier transform limit, we can assume that pulses have negligible chirp. This fact allows us to use the Wiener–Khinchin theorem to obtain field autocorrelation trace performing fast Fourier transform of each single-shot spectrum [Figs. 2(b) and 2(d)]. The formation dynamics features four transition stages, starting from modulation instability (Stage I), sequentially undergoing through breathing dynamics (Stage II) and formation of multi-peak structures (Stage III) to final mode-locking generation (Stage IV). Figures 2(a)–2(d) demonstrate typical single-shot spectra and field autocorrelation traces, corresponding to each of the four states of the pulse build-up process: at round-trip numbers 150 (Stage I), 350 (Stage II), 650 (Stage III), and 1200 (Stage IV). Visualization 1 and Visualization 2 demonstrate more detailed spectral evolution and field autocorrelation dynamics of pulses over formation stages.

The initial Stage I of the formation evolution (up to ∼250th round trip) presents instability dynamics, similar to the one observed in unidirectional ring fiber and Kerr-lens mode-locked solid-state lasers [6,7,22]. It should be noted that such intensity fluctuations do not represent any information in the spectral domain, but correspond to picosecond oscillations of continuous-wave radiation in the time domain [6]. A group of narrowband oscillations are combining into an unstable broad

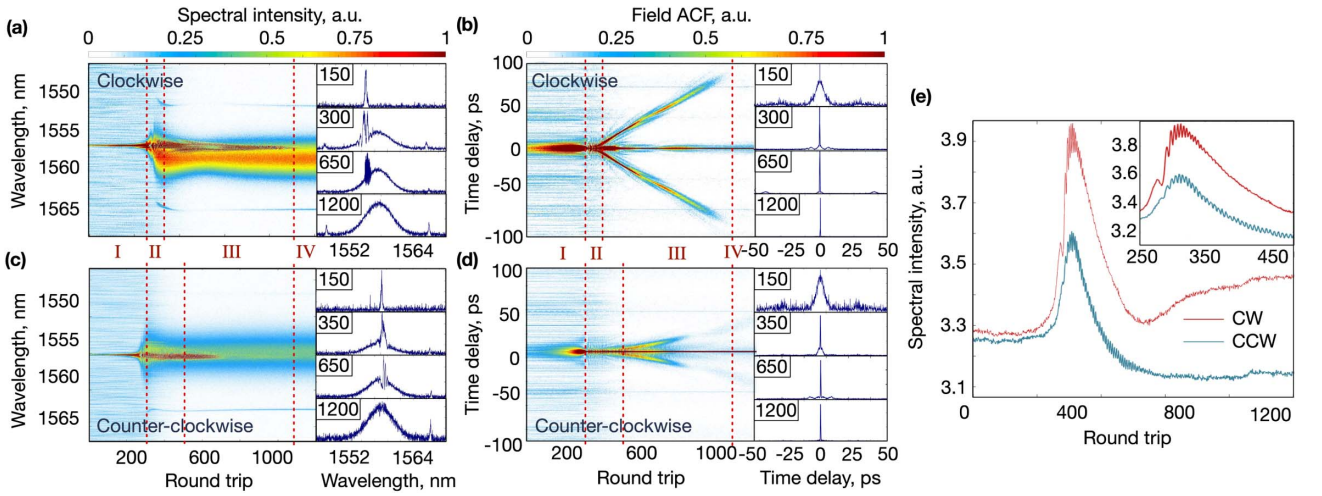

Fig. 2. Experimental results of the build-up of bidirectional solitons: clockwise (top) and counter-clockwise (bottom) (see Visualization 1 and Visualization 2). (a),(c) The real-time spectral and (b),(d) the field autocorrelation evolution with the characteristic cross sections. (e) Energy evolution of clockwise (CW) and counter-clockwise (CCW) pulses. Inset: breathing dynamics zoom-in.

pulse [7]. There is a minor delay in the mode-locking start-up of counter-propagating pulses. First, the clockwise pulse starts its formation from the instability (250 round trip), while the counter-clockwise pulse catches up after ∼15 round trips.

Analysis of the arrival time of counter-propagating pulses on photodetectors and mapping the events to the laser setup geometry have confirmed that both pulses originate in the SWNT saturable absorber, as predicted in Refs. [16,19]. Collision points in the laser cavity are static at Stage I. However, with further evolution to Stage II the trajectories of the pulses tilt, indicating that the colliding points start moving around the laser cavity with the repetition rate of 105.8 Hz, which constitutes the repetition frequency difference of counter-propagating pulses [17]. We refer it to the intensity discriminated transmission of the nonlinear polarization evolution modulator. Appropriate settings of polarization controllers in the laser cavity create a difference in counter-propagating pulse intensities and, therefore, distinct effective refractive indices and, in the end, a difference of optical paths in the cavity for counter-propagating pulses.

With the transition to Stage II of the pulse formation, spectra of both pulses obtain significant broadening. This is justified by the field autocorrelation evolution, showing the formation of a dominant high-intensity femtosecond peak [Figs. 2(b) and 2(d)]. At the same time, pronounced Kelly sidebands originate in the spectra of counter-propagating pulses [Figs. 2(a) and 2(c)]. Still, the formation of dominant pulses does not correspond to establishing steady-state mode-locking. Figure 2(e) shows that the energy of pulses, calculated as integrated spectral intensity, experiences rapid increase over 30 round trips to its maximum, followed by a slow relaxation. The magnified inset in Fig. 2(e) demonstrates the pulse energy dynamics around its maximum, showing pronounced modulation. Such energy modulation is characteristic for pulse breathing dynamics, which is clearly observed in Fig. 3, showing zoom-in dynamics of counter-propagating pulses at Stage II. 2D maps of spectral evolution [Figs. 3(a) and 3(c)] demonstrate

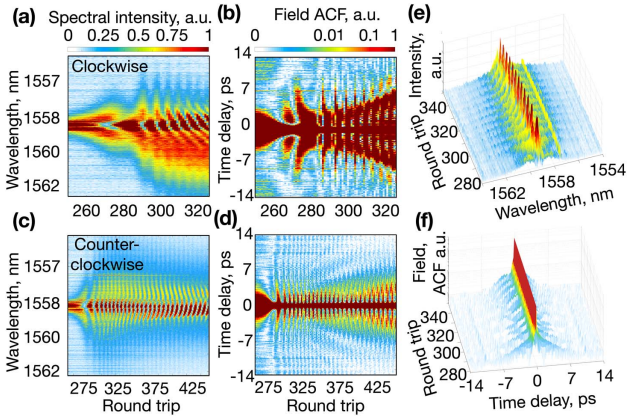

Fig. 3. Stage III: Breathing dynamics. (a),(c) Single-shot spectra and (b),(d) field autocorrelation evolution. Detailed dynamics of (e) counter-clockwise single-shot pulse spectrum and (f) field autocorrelation.

central intensity oscillating from its maximum to minimum value, while fringing patterns feature negligible tilt. The absence of tilt indicates that there is no change of the relative phase between main and breathing pulse edges. Indeed, the field autocorrelation evolution [Figs. 3(b) and 3(d)] shows non-diverging breathing dynamics of pulse edges. The counter-clockwise pulse experiences breathing over 150 round trips, which allows a more detailed study of the fringing pattern, further depicted in Figs. 3(e) and 3(f). In comparison, the clockwise pulse evolves to the next Stage III of the build-up process with the spectral intensity decrease within only ∼30 round trips.

The spectral evolution of counter-propagating pulses at Stage III and their typical single-shot spectra, presented in Figs. 2(a) and 2(c), demonstrate a modulation pattern close at the top of the spectrum. It is worth noticing that only part of the spectrum is modulated. Figures 2(a) and 2(c) show that

spectra of the clockwise pulse feature modulation fringes positioned at ~2 nm toward shorter wavelengths from the central peak. In contrast, modulation of counter-clockwise pulse spectra is ~0.4 nm redshifted. The shape of spectra indicates the formation of multi-peak structures of different duration, whose interference produces a modulated pattern. Indeed, starting from ~330 and ~450 round trips pulse quantization becomes well-observed for clockwise and counter-clockwise, correspondingly (see Visualization 2). Breathing edges of the field autocorrelation in Stage II break into several individual peaks of picosecond duration in both counter-propagating channels [Figs. 2(b) and 2(d)]. Intensities of the main peaks are tenfold higher than that of subordinate peaks. Such dynamics differ from the observed bound-solitons formation of ultrashort pulse build-up in unidirectional lasers [7]. The spectral position of modulation and duration of subordinate pulses have evolved from the original seed pulse from Stage I. Subordinate peaks do not feature balanced attraction to the main peak and, therefore, diverge from the central pulse. The rapid increase of separation causes a change of the multiple peaks phase. Therefore, the spectral interference pattern changes, and the modulation period is decreasing. In Figs. 2(a) and 2(c), Stage III depicts pronounced tilt of spectral modulation fringes. At later stages of formation dynamics, more subordinate peaks are formed, justified by the multi-peak structure of the field autocorrelation functions in both directions [Figs. 2(b) and 2(d)]. Nevertheless, these multi-pulse complexes vanish with further evolution over round trips. Major subordinate pulses got annihilated after ~1100 round trips in both generation directions.

As we introduced above, the comprehensive understanding of counter-propagating soliton interactions experiences a shortage in efficient numerical models. Few discrete studies have been discussing the nature of collision of counter-propagating ultrashort pulses in media [20,23]. These theoretical works showed that interaction of counter-propagating pulses is not integrable and, therefore, does not produce a soliton solution. The result of pulse collision strongly depends on initial conditions of each colliding pulse, such as duration or group velocity, as well as their relative polarization. Thus, Afanas'ev *et al.* have determined the result of ultrashort pulse collision in a resonant two-level medium in regards to their peak powers, demonstrating that low-intensity components got annihilated, while collision of relatively high-peak-power pulses leads to a portion of their energy to transfer to low-intensity secondary diverging pulses, as oscillating "tails" of the primary pulse. In Ref. [23] the authors considered different relative polarization of colliding pulses and numerically predicted the formation of secondary solitary waves for pulses with orthogonal polarization states and formation of population grating in the interaction region in the case of parallel states of polarization. Our experimental studies verify this theoretical observation by the demonstration of different build-up dynamics of counter-propagating pulses, depending on the initial conditions (compared with Ref. [24]). We assert that the collision of counter-propagating pulses in the laser cavity plays a pivotal role in the formation of multi-soliton structures and their further annihilation during the build-up process of steady-state mode-locking in a bidirectional fiber laser. Therefore, counter-propagating pulses with evolving intensities and polarization states experience different formation dynamics in the cavity.

4. SUMMARY

In conclusion, we have recorded the real-time formation dynamics of counter-propagating solitons in the bidirectional mode-locked erbium-doped fiber laser. By using the DFT technique, we have analyzed transient fast dynamics during soliton build-up toward the stable bidirectional mode-locking regime. Although counter-propagating pulses experience a similar evolution pattern, they undergo through each evolution stage over a different time period. The difference in evolution matches the difference in intensities: domination of the clockwise channel and suppression of counter-clockwise pulses. Therefore, we can conclude that counter-propagating pulses build up independently.

We experimentally observed that the primary pulse in each direction is formed from modulation instability transitions through two key build-up stages of breathing and subordinate pulse formation into conventional stable solitons. In comparison to earlier demonstrated results on unidirectional pulse formation [6,7], soliton molecules structures have not been observed in either of the directions. In contrast, subordinate divergent peak intensities are present in the formation dynamics, which is referred to as the inelastic collision of counter-propagating pulses. When the intensity of such subordinate peaks reaches the threshold, they annihilate, leaving main soliton pulses oscillating in the cavity.

We extrapolate that underlying phenomena of rich nonlinear dynamics during pulse formation in bidirectional fiber lasers affect not only formation evolution of pulses but also steady-state mode-locked operation. The previous studies of this laser configuration in Ref. [17] demonstrated two bidirectional regimes with pulses generated at slightly different repetition rates. Further studies of nascent stages of the build-up have revealed various possible build-up scenarios, e.g., through Q-switched instabilities [24], which have highlighted the critical role of polarization settings in pulse formation mechanisms and laser operating regimes. Our findings also demonstrate that the net cavity dispersion is an important factor in the formation dynamics. Thus, the earlier work of Yu *et al.* discussed the build-up process in net-normal dispersion bidirectional lasers and demonstrated the similarities of dynamics of counter-propagated beams during their build-up [19]. This is the polar opposite to the results demonstrated here, as we justify that pulses evolve independently through formation Stages I to IV. We believe that our studies provide the basis for further investigation of pulse formation and evolution in nonlinear bidirectional laser systems, which will pave the way to understand underlying physical phenomena. Therefore, comprehensive knowledge on the overall dynamics will result in transforming bidirectional ultrafast lasers into robust and versatile tools for gyroscopy and spectroscopy and a range of emerging applications.

Funding. Royal Academy of Engineering and Global Challenges Research Fund; H2020 Marie Skłodowska-Curie Actions (COFUND-MULTIPLY).

Disclosures. The authors declare no conflicts of interest.

REFERENCES

1. E. Turitsyna, S. Smirnov, S. Sugavanam, N. Tarasov, X. Shu, S. Babin, E. Podivilov, D. Churkin, G. Falkovich, and S. Turitsyn, "The laminar-turbulent transition in a fibre laser," Nat. Photonics **7**, 783–786 (2013).
2. M. Närhi, B. Wetzel, C. Billet, S. Toenger, T. Sylvestre, J.-M. Merolla, R. Morandotti, F. Dias, G. Genty, and J. M. Dudley, "Real-time measurements of spontaneous breathers and rogue wave events in optical fibre modulation instability," Nat. Commun. **7**, 13675 (2016).
3. K. Krupa, K. Nithyanandan, U. Andral, P. Tchofo-Dinda, and P. Grelu, "Real-time observation of internal motion within ultrafast dissipative optical soliton molecules," Phys. Rev. Lett. **118**, 243901 (2017).
4. G. Herink, F. Kurtz, B. Jalali, D. R. Solli, and C. Ropers, "Real-time spectral interferometry probes the internal dynamics of femtosecond soliton molecules," Science **356**, 50–54 (2017).
5. J. Peng, S. Boscolo, Z. Zhao, and H. Zeng, "Breathing dissipative solitons in mode-locked fiber lasers," Sci. Adv. **5**, eaax1110 (2019).
6. G. Herink, B. Jalali, C. Ropers, and D. Solli, "Resolving the build-up of femtosecond mode-locking with single-shot spectroscopy at 90 MHz frame rate," Nat. Photonics **10**, 321–326 (2016).
7. J. Peng, M. Sorokina, S. Sugavanam, N. Tarasov, D. V. Churkin, S. K. Turitsyn, and H. Zeng, "Real-time observation of dissipative soliton formation in nonlinear polarization rotation mode-locked fibre lasers," Commun. Phys. **1**, 20 (2018).
8. C. Lapre, C. Billet, F. Meng, P. Ryczkowski, T. Sylvestre, C. Finot, G. Genty, and J. M. Dudley, "Real-time characterization of spectral instabilities in a mode-locked fibre laser exhibiting soliton-similariton dynamics," Sci. Rep. **9**, 13950 (2019).
9. K. Goda and B. Jalali, "Dispersive Fourier transformation for fast continuous single-shot measurements," Nat. Photonics **7**, 102–112 (2013).
10. A. Tikan, S. Bielawski, C. Szwaj, S. Randoux, and P. Suret, "Single-shot measurement of phase and amplitude by using a heterodyne time-lens system and ultrafast digital time-holography," Nat. Photonics **12**, 228–234 (2018).
11. P. Ryczkowski, M. Närhi, C. Billet, J.-M. Merolla, G. Genty, and J. M. Dudley, "Real-time full-field characterization of transient dissipative soliton dynamics in a mode-locked laser," Nat. Photonics **12**, 221–227 (2018).
12. Z. Wang, K. Nithyanandan, A. Coillet, P. Tchofo-Dinda, and P. Grelu, "Optical soliton molecular complexes in a passively mode-locked fibre laser," Nat. Commun. **10**, 830 (2019).
13. M. Yoshizawa and T. Kobayashi, "Experimental and theoretical studies on colliding pulse mode locking," IEEE J. Quantum Electron. **20**, 797–803 (1984).
14. K. Kieu and M. Mansuripur, "All-fiber bidirectional passively mode-locked ring laser," Opt. Lett. **33**, 64–66 (2008).
15. M. Chernysheva, M. A. Araimi, H. Kbashi, R. Arif, S. V. Sergeyev, and A. Rozhin, "Isolator-free switchable uni- and bidirectional hybrid mode-locked erbium-doped fiber laser," Opt. Express **24**, 15721–15729 (2016).
16. A. A. Krylov, D. S. Chernykh, and E. D. Obraztsova, "Gyroscopic effect detection in the colliding-pulse hybridly mode-locked erbium-doped all-fiber ring soliton laser," Opt. Lett. **42**, 2439–2442 (2017).
17. M. Chernysheva, S. Sugavanam, and S. Turitsyn, "Real-time observation of the optical Sagnac effect in ultrafast bidirectional fibre lasers," APL Photonics **5**, 016104 (2020).
18. T. Ideguchi, T. Nakamura, Y. Kobayashi, and K. Goda, "Kerr-lens mode-locked bidirectional dual-comb ring laser for broadband dual-comb spectroscopy," Optica **3**, 748–753 (2016).
19. Y. Yu, C. Kong, B. Li, J. Kang, Y.-X. Ren, Z.-C. Luo, and K. K. Wong, "Behavioral similarity of dissipative solitons in an ultrafast fiber laser," Opt. Lett. **44**, 4813–4816 (2019).
20. A. Afanas'ev, V. Volkov, V. Dritz, and B. Samson, "Interaction of counter-propagating self-induced transparency solitons," J. Mod. Opt. **37**, 165–170 (1990).
21. M. J. Shaw and B. W. Shore, "Collisions of counterpropagating optical solitons," J. Opt. Soc. Am. B **8**, 1127–1134 (1991).
22. X. Liu, D. Popa, and N. Akhmediev, "Revealing the transition dynamics from Q-switching to mode locking in a soliton laser," Phys. Rev. Lett. **123**, 093901 (2019).
23. A. Pusch, J. M. Hamm, and O. Hess, "Controllable interaction of counterpropagating solitons in three-level media," Phys. Rev. A **82**, 023805 (2010).
24. I. S. Kudelin, S. Sugavanam, and M. Chernysheva, "Build-up of bidirectional ultrashort pulse laser generation: from Q-switched instabilities to mode-locking," in *European Conference on Lasers and Electro-Optics* (Optical Society of America, 2019), paper cj_7_1.